

Scaling of temporal correlations in an attractive Tomonaga-Luttinger spin liquid

K. Yu. Povarov, D. Schmidiger, N. Reynolds, and A. Zheludev

Neutron Scattering and Magnetism, Laboratory for Solid State Physics, ETH Zürich, Switzerland

R. Bewley

ISIS Facility, Rutherford Appleton Laboratory, Chilton, Didcot, Oxon OX11 0QX, United Kingdom

(Dated: December 3, 2024)

We report temperature-dependent neutron scattering measurements of the local dynamic structure factor in the quantum spin ladder $(\text{C}_7\text{D}_{10}\text{N})_2\text{CuBr}_4$ in a magnetic field $H = 9$ T, in its gapless quantum-critical phase. We show that the measured quantity has a scaling form consistent with expectations for a Tomonaga-Luttinger liquid with attraction. The measured Luttinger parameter $K \approx 1.25$ and scaling function are in excellent agreement with first principles DMRG calculations for the underlying spin Hamiltonian.

PACS numbers: 75.10.Kt, 75.10.Jm, 75.40.Gb, 78.70.Nx

Landau's Fermi liquid theory is the basis of our understanding of interacting fermions, be it metals or neutron stars [1–4]. Landau's main argument regarding the stability of quasiparticles breaks down in low dimensions. Interestingly, in one dimension, interacting fermions still bear a unified description, known as the Tomonaga-Luttinger liquid (TLL) [5–8]. All low-energy properties of such fermions, including thermodynamics, correlation functions, susceptibilities, etc., are predicted to be *universal* in that any details of the interaction potential are irrelevant. Instead, the interactions are characterized by a single dimensionless quantity, known as the Luttinger parameter K . Free fermions correspond to $K = 1$, $K < 1$ implies repulsive interactions, and fermions with attraction have $K > 1$.

Experimental validations of this astonishingly strong statement of universality are of utmost importance. The most obvious model systems are one-dimensional metals in charge-transfer salts [9], quantum wires [10] and quantum Hall effect edge states [11]. However, TLLs with the most experimentally accessible correlation functions are found in seemingly unlikely places, namely in magnetic insulators. According to Haldane's famous conjecture [12], at low energies, all gapless one-dimensional quantum spin systems can be mapped into interacting fermions. The benefit of such mapping is that spin correlations can be directly probed with neutron scattering, NMR, ESR and other techniques. A huge success of this approach were measurements of universal finite-temperature scaling laws for correlation functions in Heisenberg $S = 1/2$ -chains [13, 14]. Similar work was done on non-TLL critical systems, such as gapless spin ladders with cyclic exchange [15]. However, Heisenberg spin chains are but a very particular case of a *repulsive* TLL, with $K = 1/2$ [8, 16]. Fermions (electrons) in quantum wires and one-dimensional metals are also repulsive. Very recently, it was shown that an *attractive* TLL, where the behavior is expected to be qualitatively different, can be realized in a strong-leg $S = 1/2$ Heisenberg spin ladder in mag-

netic fields [17, 18]. In this work we use neutron spectroscopy to observe distinctive finite- T scaling of local temporal correlations in such a system. Specifically, we find that the measured scaled local dynamic structure factor $T^{1/2K-1}S(\omega)$ is a *universal* function of ω/T in wide temperature and energy ranges with $K > 1$.

Our target material, $(\text{C}_7\text{D}_{10}\text{N})_2\text{CuBr}_4$ (DIMPY for short) is arguably the best known realization of the AF $S = 1/2$ Heisenberg ladder model [17, 19–21]. The magnetic properties are due to Cu^{2+} cations linked in ladder structures by superexchange pathways via Br^- anions [20]. Organic ligands act as spacers between these ladders in the monoclinic crystal structure, providing excellent one-dimensionality. The spin Hamiltonian of DIMPY is well established through a quantitative comparison of inelastic neutron scattering spectra and thermodynamic data to first principle Density Matrix Renormalization Group (DMRG) calculations [20, 21]. The two ladder exchange constants are $J_{\parallel} = 1.42$ meV, $J_{\perp} = 0.82$ meV for the leg and rung, respectively. Inter-ladder interactions are as small as $J' \simeq 6$ μeV [17]. The ground state is a spin singlet with a gap $\Delta = 0.33$ meV. A gapless quantum-critical phase is induced in DIMPY by external magnetic fields exceeding $H_{c1} \simeq 2.6$ T [17, 18, 22].

Previous DMRG calculations have shown that above H_{c1} DIMPY is an *attractive* TLL in a wide range of fields [17]. This has recently been confirmed by NMR experiments [18]. Still, measuring the relevant temporal correlations experimentally is far from straightforward. Most of the observable spectral features are specific to spin ladder physics and are not related to TLL dynamics [22]. TLL excitations are revealed only at the lowest energies, and are barely discernible in previous measurements due to limited energy resolution. Therefore, our new experiments, while using the same sample and the LET neutron spectrometer [23] at ISIS as in previous studies [22], took advantage of a different instrument configuration with a lower neutron incident energy $E_i = 2.2$ meV. This allowed us to achieve a calculated energy resolution

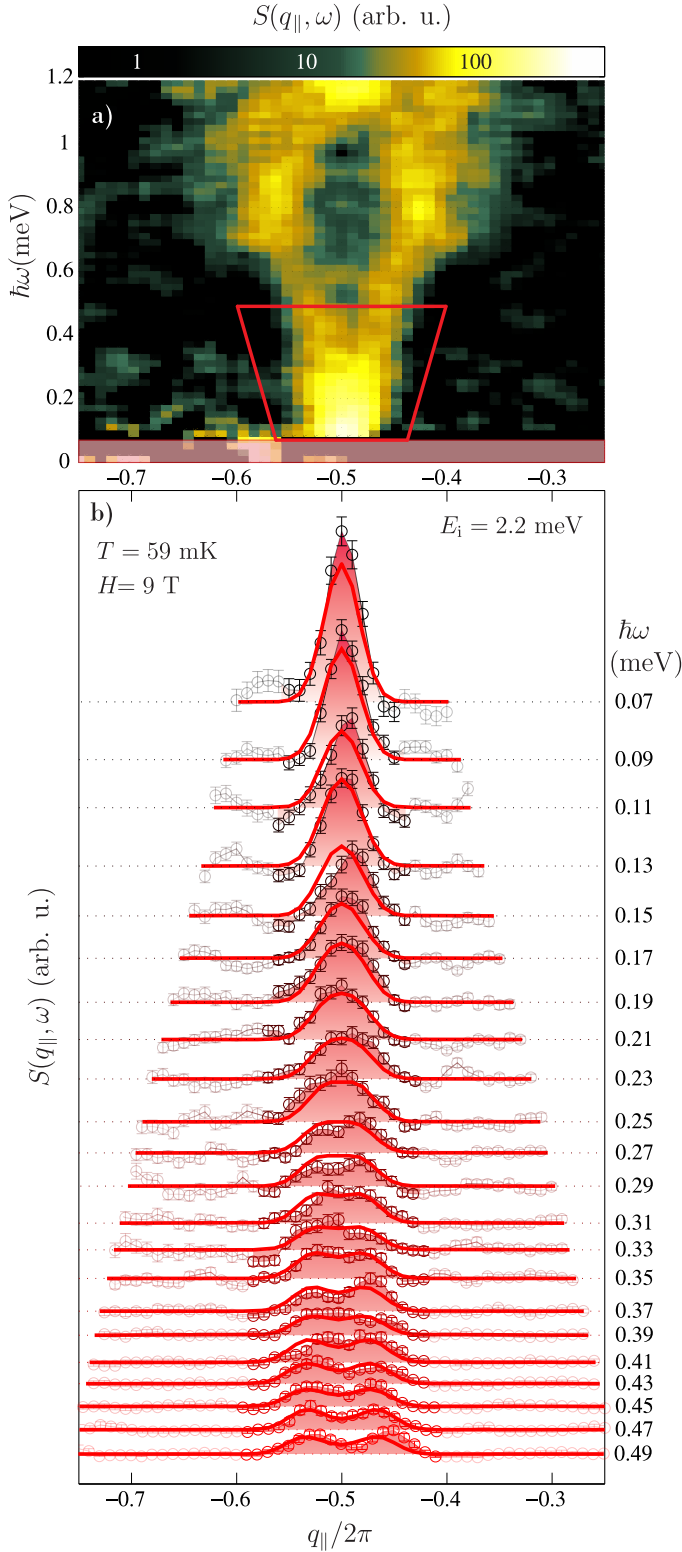


FIG. 1. Measured dynamic spin structure factor of DIMPY at $T = 59$ mK. a) False color map of $S(q_{\parallel}, \omega)$. The boundary shows the region in energy-momentum space, used in the analysis. b) Constant energy cuts with the q_{\parallel} integration range highlighted. All the data is background and structure factor corrected, as described in the text. Solid lines correspond to the TLL theoretical prediction convoluted with the spectrometer resolution.

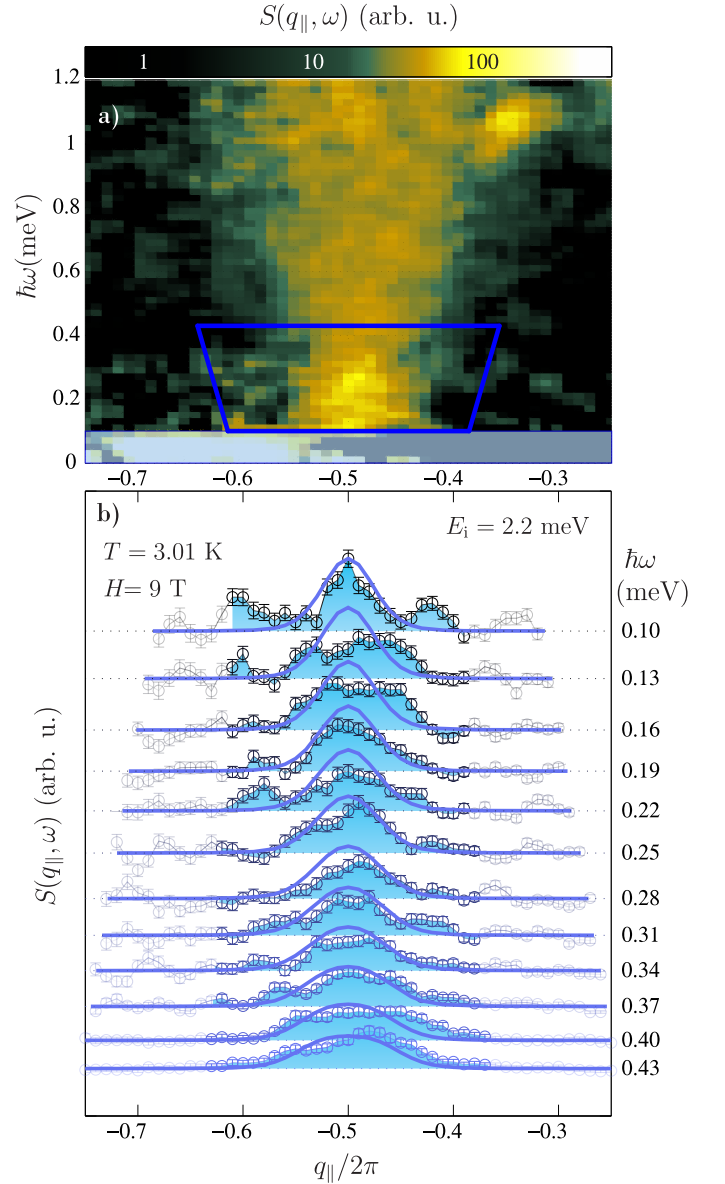


FIG. 2. As Fig. 1, for $T = 3.01$ K.

of $\delta E \sim 20\text{--}30\text{ }\mu\text{eV}$, depending on energy transfer. Typical data collected at $H = 9$ T and $T = 59$ mK in this mode are shown in Fig. 1a. The false color plot is that of the dynamic structure factor $S(q_{\parallel}, \omega)$, where $q_{\parallel} = (\mathbf{Q} \cdot \mathbf{a})$ is the momentum transfer along the crystallographic a axis (along the ladder legs). As explained in detail in Refs. [20, 21], these data almost entirely show antisymmetric ladder correlations.

Previous DMRG calculations identified all the main components of the excitation spectrum [22]. Thus, we know that the prominent gapped incommensurate excitations seen at $H = 9$ T at around ≈ 0.8 meV energy transfer are due to longitudinal spin correlations S^{zz} and are not TLL-related. Since they can not be avoided in

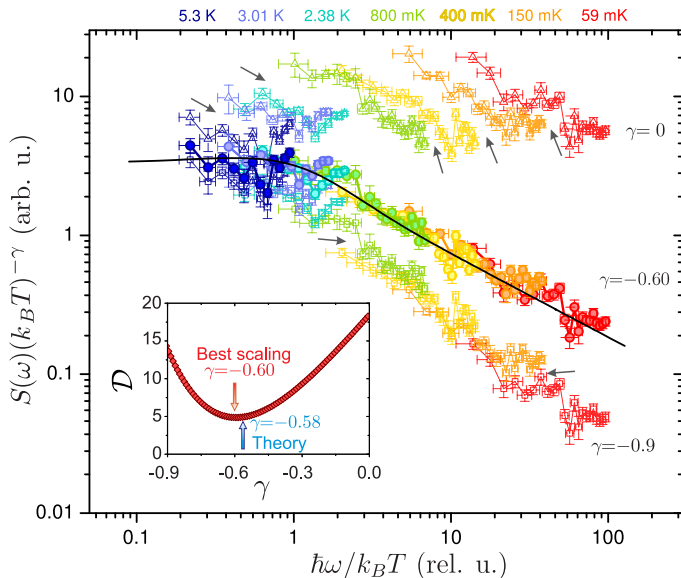


FIG. 3. Local dynamic structure factor $S(\omega)$ measured in DIMPY at $H = 9$ T at several temperatures, plotted in the scaling representation with different scaling exponents γ . Arrows mark the apparent violations of scaling for non-optimal values of γ . The solid line is the exact TLL scaling function F (Eq. 1) with the Luttinger parameter $K = 1.25$, corresponding to $\gamma = -0.6$. Inset: γ -dependence of data overlap function \mathcal{D} (Eq. 2).

the experiment, in our analysis we shall only consider the data below 0.5 meV energy transfer. The scattering at these low energies is a V-shaped continuum visible in Fig. 1a around the commensurate point $q_{\parallel} = \pi$. It is due to correlations between transverse spin components with the corresponding structure factor $S^{\pm\mp}$ [22]. This structure factor is representative of TLL correlations, and is the main focus of this study. The slope of the lower bound of the observed continuum corresponds to the Fermi velocity of the TLL. The experimental value $u = 1.98 \pm 0.02$ meV is in excellent agreement with the DMRG result $u = 1.91$ meV [24] for DIMPY at $H = 9$ T [17]. DMRG additionally predicts incommensurate gapless excitations centered around $q_{\parallel} = \pi(1 \pm 0.36)$. However, their intensity is calculated to be two orders of magnitude smaller numerically, and they are not visible experimentally. In our analysis this contribution to low-energy scattering will be disregarded.

Having chosen a suitable measurement window and identified the relevant inelastic neutron scattering signal, we still need to ensure that the TLL mapping remains valid in that range. The essence of the TLL model are i) a linear dispersion relation for the fermions and ii) an infinitely deep Fermi sea. It is a valid approximation only if the experimental energy transfers and temperature do not probe the actual Fermi sea too deeply or extend to non-linear dispersion regimes. Looking at

previous DMRG calculations for $S^{\pm\mp}(q_{\parallel}, \omega)$ at a similar field $H = 7$ T, we conclude that in our case i) holds to at least 1 meV energy transfer. At $H = 9$ T the depth of the Fermi sea is $\Delta_F = g\mu_B(H - H_{c1}) \sim 0.77$ meV. Since we have already limited ourselves to excitations below 0.5 meV, the TLL model should be applicable with a good safety margin, as long as we also limit the experimental temperatures to $T < 5$ K ~ 0.5 meV/ k_B .

Constant-energy cuts from two data sets collected at base temperature and at $T = 3$ K are shown in Figs. 1b and 2b, respectively. Here the background, measured in zero applied field at base temperature, as described in Ref. [22], was subtracted. In addition, the intensity was corrected for the magnetic form factors of the spin ladder and Cu^{2+} ions. At $H = 9$ T, the finite momentum resolution of our experiments prevents us from discerning any internal structure of the excitation continuum below 0.25 meV energy transfer. As done previously for $S = 1/2$ chain systems [13, 25, 26], this problem was entirely avoided by integrating the dynamic structure factor over q_{\parallel} . The integration range was limited to the trapezoidal areas indicated in Figs. 1a and 2a, to avoid picking up additional noise. The resulting momentum-integrated structure factor is the *local* temporal transverse spin correlation function in frequency representation $S^{\pm\mp}(\omega)$. It is similar to the quantity obtained from $1/T_1$ NMR relaxation rates, except that the latter corresponds to a single very low energy transfer. In contrast, our $S^{\pm\mp}(\omega)$ data reliably cover the range 0.07–0.5 meV and were collected at temperatures 0.06–5 K.

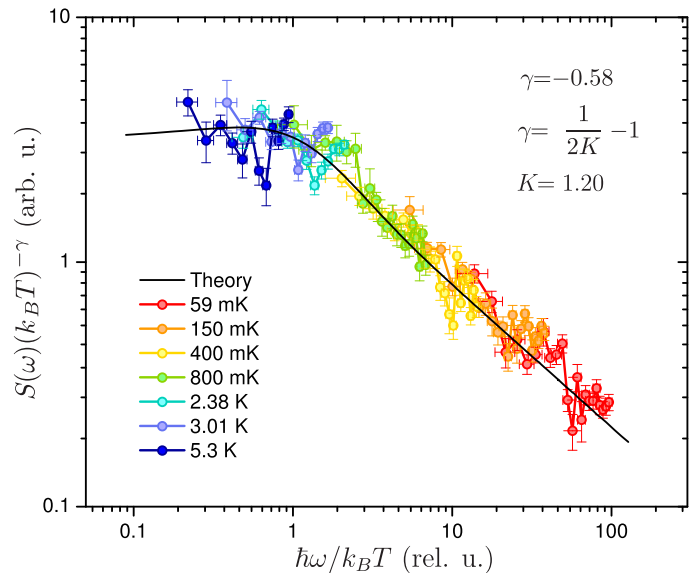


FIG. 4. As in Fig. 3, with the scaling exponent $\gamma = -0.58$ ($K = 1.20$) derived from the Heisenberg spin Hamiltonian of DIMPY at $H = 9$ T using first principles DMRG calculations [17].

We chose to analyze these data in two separate stages. First, we consider the temperature dependence of the measured structure factor without referring to specific results for the TLL. In fact, our only starting consideration is that the magnetized spin ladder is in a quantum critical state [27], and that $S^{\pm\mp}$ is precisely the critical correlation function. In this case, the only relevant energy scale is temperature itself, so that the *shape* of $S^{\pm\mp}$ is a function of single variable of ω/T . One can then expect the following scaling form for this quantity [28]:

$$S^{\pm\mp}(\omega) = (k_B T)^\gamma F(\hbar\omega/k_B T). \quad (1)$$

If so, with an appropriate choice of the scaling exponent γ we should observe a data collapse for measurements collected at different temperatures. For illustration purposes, Fig. 3a shows scaling plots of our data obtained with three different exponents. For $\gamma = 0$ and $\gamma = -0.9$ there is obviously no data collapse, the data discontinuities being indicated by arrows. To find the “best” scaling exponent, we introduced an *ad hoc* measure of the quality of data overlap

$$\mathcal{D} = \sum_{n,i,j} \frac{(\sigma_{n,i} - \sigma_{n+1,j})^2}{(\Delta\sigma_{n,i} + \Delta\sigma_{n+1,j})^2} \cdot \frac{1}{\sum_{n,i,j}}, \quad (2)$$

where $\sigma_{n,i} = S(T_n, \omega_{ni})/(k_B T_n)^\gamma$, i, j enumerate the nearest-neighbor pairs of points in data subsets T_n and T_{n+1} , and $\Delta\sigma_{n,i}$ is the corresponding error. Figure 3 inset shows the γ -dependence of \mathcal{D} . The best data collapse is obtained with $\gamma = -0.60$, as indicated by the arrow in Figure 3 inset. The corresponding scaling plot of $S^{\pm\mp}$ is shown in solid symbols in Fig. 3 main panel. An excellent overlap between data sets collected at different temperatures is apparent.

Having established the scaling form of the local dynamic structure factor experimentally, we can compare the result to predictions of TLL theory. In this model the dynamic structure factor scales with a known scaling function and exponent [8, 28]:

$$S^{\pm\mp}(q_{\parallel}, \omega) \propto T^{1/2K-2} \times \Im \left[\left(1 - \exp\left(-\frac{\hbar\omega}{k_B T}\right) \right)^{-1} \Phi\left(\frac{\hbar\omega}{k_B T}, \frac{u(q_{\parallel} - \pi)}{k_B T}\right) \right],$$

$$\Phi(x, y) = \frac{\Gamma(\frac{1}{8K} - i\frac{x-y}{4\pi})}{\Gamma(1 - \frac{1}{8K} - i\frac{x-y}{4\pi})} \frac{\Gamma(\frac{1}{8K} - i\frac{x+y}{4\pi})}{\Gamma(1 - \frac{1}{8K} - i\frac{x+y}{4\pi})}. \quad (3)$$

Integrating over momentum, and comparing this to Eq. 1 yields $\gamma = \frac{1}{2K} - 1$. From the experimentally determined scaling exponent γ we then get $K \approx 1.25$. Thus, we are dealing with one-dimensional fermions *with attraction*: $K > 1$. The comparison with TLL theory can be taken further. By integrating the function Φ in Eq. 3 numerically, using $K = 1.25$ and an arbitrary overall scale

factor, we get the solid line shown in Fig. 3a, to illustrate the excellent agreement between experiment and the TLL model.

Our precise understanding of the spin Hamiltonian for DIMPY allows us to make a direct comparison of our experimental findings to first-principles calculations. Using the field dependence of the Luttinger parameter previously calculated for DIMPY using DMRG [17], for $H = 9$ T we get $K = 1.20$ or, equivalently, $\gamma = -0.58$. This first-principles scaling exponent is very close to our *ad hoc* experimental estimate. In fact, it gives a data collapse that is almost as good. The scaling plot of our data made using the first-principles value is shown in Fig. 4. For comparison, in Fig. 4, the solid line is the theoretical scaling function F , as obtained by integrating Eq. 3, using the DMRG result for K .

Equation 3 can now be used to model the entire energy and wave vector dependent scattering intensity measured in our experiments. Numerically convoluting the analytical expression with the calculated spectrometer resolution, we get constant-energy cuts shown in solid lines in Figs. 1b and 2b. Note that the only adjustable parameter in this fit is a single overall scaling factor for all temperatures and energies. Considering the experimental noise and systematic errors due to background subtraction, the level of agreement with experiment is remarkable.

In summary, we show that the local dynamic structure factor for a magnetized strong-leg quantum spin ladder has a finite-temperature scaling form expected for a quantum-critical system. The experimentally determined scaling exponent and scaling function are in excellent agreement with those for an *attractive* Tomonaga-Luttinger liquid. In fact, the results are fully consistent with first principles calculations for the particular model spin Hamiltonian of the target compound.

We would like to emphasize that neutron scattering experiments with energy resolution, intensity and signal to background ratios necessary for such studies were enabled only very recently by major breakthroughs in neutron instrumentation at user facilities such as ISIS. This work was supported by the Swiss National Science Foundation, Division 2. AZ would like to thank Prof. Giamarchi and Prof. Essler for numerous enlightening discussions on the subject of critical dynamics.

-
- [1] L. D. Landau, Sov. Phys. - JETP **3**, 920 (1957).
 - [2] L. D. Landau, Sov. Phys. - JETP **8**, 70 (1959).
 - [3] E. M. Lifshitz and L. P. Pitaevskii, *Statistical Physics: Theory of the Condensed State* (Elsevier, 1980).
 - [4] A. A. Abrikosov, *Fundamentals of the theory of metals* (North-Holland, 1988).
 - [5] S. Tomonaga, Progress of Theoretical Physics **5**, 544 (1950).
 - [6] J. Luttinger, Journal of Mathematical Physics **4**, 1154

- (1963).
- [7] D. C. Mattis and E. H. Lieb, *Journal of Mathematical Physics* **6**, 304 (1965).
 - [8] T. Giamarchi, *Quantum Physics in One Dimension* (Clarendon Press, 2004).
 - [9] F. Zwick, S. Brown, G. Margaritondo, C. Merlic, M. Onellion, J. Voit, and M. Grioni, *Phys. Rev. Lett.* **79**, 3982 (1997).
 - [10] A. Yacoby, H. L. Stormer, N. S. Wingreen, L. N. Pfeiffer, K. W. Baldwin, and K. W. West, *Phys. Rev. Lett.* **77**, 4612 (1996).
 - [11] A. M. Chang, L. N. Pfeiffer, and K. W. West, *Phys. Rev. Lett.* **77**, 2538 (1996).
 - [12] F. D. M. Haldane, *Phys. Rev. Lett.* **45**, 1358 (1980).
 - [13] D. C. Dender, *Spin Dynamics in the Quasi-One-Dimensional $S = 1/2$ Heisenberg Antiferromagnet Copper Benzoate*, Ph.D. thesis, Johns Hopkins University (1997).
 - [14] B. Lake, D. A. Tennant, C. D. Frost, and S. E. Nagler, *Nature Materials* **4**, 329 (2005).
 - [15] B. Lake, A. M. Tsvelik, S. Notbohm, D. A. Tennant, T. G. Perring, M. Reehuis, C. Sekar, G. Krabbes, and B. Büchner, *Nature Physics* **6**, 50 (2010).
 - [16] H. J. Schulz, *Phys. Rev. B* **34**, 6372 (1986).
 - [17] D. Schmidiger, P. Bouillot, S. Mühlbauer, S. Gvasaliya, C. Kollath, T. Giamarchi, and A. Zheludev, *Phys. Rev. Lett.* **108**, 167201 (2012).
 - [18] M. Jeong, H. Mayaffre, C. Berthier, D. Schmidiger, A. Zheludev, and M. Horvatić, *Phys. Rev. Lett.* **111**, 106404 (2013).
 - [19] T. Hong, Y. H. Kim, C. Hotta, Y. Takano, G. Tremelling, M. M. Turnbull, C. P. Landee, H.-J. Kang, N. B. Christensen, K. Lefmann, K. P. Schmidt, G. S. Uhrig, and C. Broholm, *Phys. Rev. Lett.* **105**, 137207 (2010).
 - [20] D. Schmidiger, S. Mühlbauer, S. N. Gvasaliya, T. Yankova, and A. Zheludev, *Phys. Rev. B* **84**, 144421 (2011).
 - [21] D. Schmidiger, P. Bouillot, T. Guidi, R. Bewley, C. Kollath, T. Giamarchi, and A. Zheludev, *Phys. Rev. Lett.* **111**, 107202 (2013).
 - [22] D. Schmidiger, S. Mühlbauer, A. Zheludev, P. Bouillot, T. Giamarchi, C. Kollath, G. Ehlers, and A. M. Tsvelik, *Phys. Rev. B* **88**, 094411 (2013).
 - [23] R. Bewley, J. Taylor, and S. Bennington, *Nucl. Instrum. Methods Phys. Res., Sect. A* **637**, 128 (2011).
 - [24] Since q_{\parallel} is dimensionless in our notation, velocity is measured in energy units, so that $\hbar\omega = uq_{\parallel}$ for a linear dispersion relation.
 - [25] A. Zheludev, T. Masuda, G. Dhalenne, A. Revcolevschi, C. Frost, and T. Perring, *Phys. Rev. B* **75**, 054409 (2007).
 - [26] G. Simutis, S. Gvasaliya, M. Månsson, A. L. Chernyshev, A. Mohan, S. Singh, C. Hess, A. T. Savici, A. I. Kolesnikov, A. Piovano, T. Perring, I. Zaliznyak, B. Büchner, and A. Zheludev, *Phys. Rev. Lett.* **111**, 067204 (2013).
 - [27] S. Sachdev, T. Senthil, and R. Shankar, *Phys. Rev. B* **50**, 258 (1994).
 - [28] S. Sachdev, *Quantum Phase Transitions* (John Wiley & Sons, Ltd, 2007).